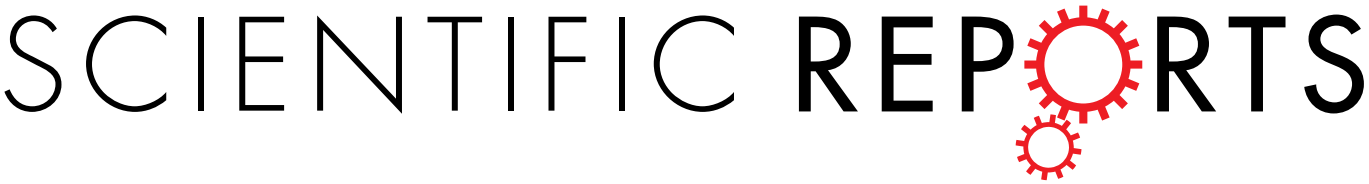

OPEN

Received: 18 January 2016
Accepted: 06 May 2016
Published: 27 May 2016

Dependences of Q-branch integrated intensity of linear-molecule pendular spectra on electric-field strength and rotational temperature and its potential applications

Min Deng, Hailing Wang, Qin Wang & Jianping Yin

We calculate the pendular-state spectra of cold linear molecules, and investigated the dependences of "Q-branch" integrated intensity of pendular spectra on both electric-field strength and molecular rotation-temperature. A new multi-peak structure in the "Q-branch" spectrum is appearing when the Stark interaction strength $\omega = \mu E/B$ equal to or larger than the critical value. Our study shows that the above results can be used not only to measure the electric-field vector and its spatial distribution in some electrostatic devices, such as the Stark decelerator, Stark velocity filter and electrostatic trap and so on, but also to survey the orientation degree of cold linear molecules in a strong electrostatic field.

Since a new concept on pendular states of molecules in strong electric field was first proposed in 1991[1] and the pendular-state spectra of $(HCN)_3$ in strong electric fields were first reported in 1992[2,3], theoretical[4–8] and experimental[9–14] investigations on the pendular-state properties and their spectrum structures of cold polar molecules have made a great progress. These studies show that such a novel pendular-state spectrum can be used to precisely measure molecular electric dipole moment[15,16] and its change[17], to study some new complexes, such as, NH_3CN complex[18] and CH_3---H_2O radical complex[19], and so on. In addition, oriented cold/ultracold polar molecules have important applications in quantum information science[20], biochemistry, and biophysics[21].

However, how to prepare cold/ultracold molecules is a very important scientific question and has become one of hot points in the fields of atomic, molecular and optical physics (AMO), quantum dipole gases and quantum information science. cold/ultracold molecules attract great interests of scientists to prepare and study them because they have many important applications in cold collisions and cold chemistry, molecular BEC (Bose-Einstein condensate) and Fermi quantum degeneration, quantum and nonlinear molecule optics, cold molecular spectroscopy and precise measurement, integrated molecule optics and molecule chip, quantum computing and information processing, and so on. Particularly, cold/ultracold polar molecules can be used to study their quantum-state controlled pendular spectrum. Currently, they can be prepared and manipulated by using some electrostatic devices, such as Stark decelerator[22] and velocity filter[23,24], electrostatic guide[25] and beam splitter[26], electrostatic trap[27], and laser cooling[28,29], etc.

The accurate amplitude and direction of the electrostatic fields and their spatial distributions play important roles in the preparation and investigation of cold/ultracold molecules using above electrostatic devices[22–27]. The electric field (E-field) strength in these electrostatic devices[22–27] is varied from 0 to 100 kV cm^{-1}. Also, the measurements of externally-added the electrostatic field vector and its spatial gradient as well as the orientation degree (i.e., the polarizability) of cold heavy-atom molecules (such as YbF[30], PbF[31], PbO[32] and ThO[33], etc.) in the strong electric field play an important role in precise measurement of electron electric polar momentum (eEDM)[30–33]. It is well known that the E-field vector and its spatial distribution are basic and important physical quantities,

State Key Laboratory of Precision Spectroscopy, Department of Physics, East China Normal University, Shanghai 200062, P. R. China. Correspondence and requests for materials should be addressed to J.Y. (email: jpyin@phy.ecnu.edu.cn)

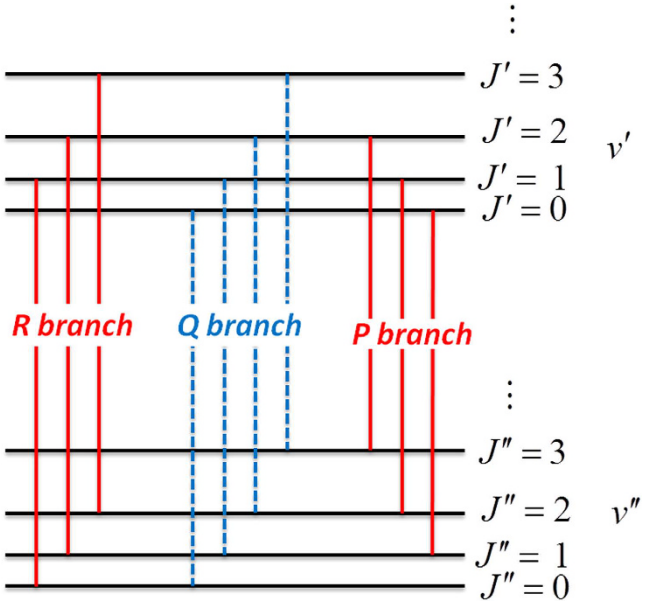

Figure 1. Energy level diagram of the pure-rovibrational band of linear $(HCCCN)_3$ with P-, R-branches (there is no Q-branch according to the selection rule).

and their measurement to date have not been solved well, unlike the measurement of the magnetic field[34]. In recent years, only a few methods have been developed to measure the E-field amplitude or the E-field vector and its spatial distribution from a weak E-field (~1 V cm^{-1}) to a moderate one (~10^3 V cm^{-1}) by using electro-optic probe[35], Stark spectrum of Rydberg-atoms[36,37] and Rydberg-molecules[38], and fluorescence-dip spectroscopy[39] and so on[40,41]. Those methods only cover a narrow range of around three orders of magnitude which is far narrower than the measuring range of the magnetic field from 10^{-15} T to 10^3 T[34]. However, the above measurement methods[35–41] cannot be used to measure *in situ* the E-field vector and its spatial distribution in the electrostatic devices[22–27] and eEDM experiments[30–33]. So it would be interesting and worthwhile to investigate the dependences of Q-branch intensity of pendular-state spectrum of cold/ultracold linear molecules on both the E-field strength and the molecular rotational temperature, and then develop a new and desirable method to measure the E-field vector and its spatial distribution with an ultra-wide surveying range. In this paper, we first present a method to calculate the pendular-state spectra of cold/ultracold linear molecules, and then study the dependences of Q-branch integrated intensity of pendular-state spectra of cold/ultracold linear molecules on both the E-field strength and the molecular rotational temperature (MRT). Also, we discuss some potential applications of the cold/ultracold linear molecule pendular-state spectrum in the measurement of the E-field vector and its spatial distribution as well as the orientation degree (i.e., the polarizability) of cold molecules. The main results and conclusions are included in final section.

Results

Calculation of pendular-state spectrum. Figure 1 shows the energy level diagram of the pure-rovibrational band of linear molecules $(HCCCN)_3$ with P-, R-branches. The Q-branch transition of $(HCCCN)_3$ is forbidden due to the selection rule. However, a so called "Q-branch" transition of the linear $(HCCCN)_3$ will appearing in an external electric field due to the mixture of the wavefunctions (i.e., due to the appearance of pendular state). Generally, polar molecules in a strong electric field will be oriented and converted from pinwheeling rotors into pendular liberators confined to oscillate over a limited angular range along the field direction. In this case, the corresponding rotation eigenstates become the pendular states. Molecules with a low rotational temperature, T, a large dipole moment, and a small molecular constant, B, are very easy to be implemented into the pendular state under a weak electric field. The pendular-state spectra were first investigated experimentally by Miller's group[3].

The pendular states are linear combinations of the field-free rotor states, $|J, M\rangle$, where J is the rotational quantum number, M is the projection of the angular momentum J along the direction of the E-filed vector[2,3]. For linear molecules with an electric dipole moment and a rotational constant B in an E-field, the ratio $\omega = \mu E(r)/B$ was used to govern the extent of hybridization of the rotor states. The Schrödinger equation of a rigid linear molecule in an E-field is given by

$$(J^2 - \omega \cos\theta)\,|\tilde{J}, M; \omega\rangle = \tilde{E}|\tilde{J}, M; \omega\rangle \quad (1)$$

where J^2 is the squared angular momentum operator, M is the projection of the angular momentum J along the E-field vector direction, and θ is the angle between the molecular axis and the E-field vector, and $\tilde{E}$ is the energy eigenvalue. The Stark eigenstate is labeled by the rotational state of the field-free case, and given by

$$|\tilde{J}, M; \omega\rangle = \sum_{J} a_{JM}(\omega)|J, M\rangle \rightarrow |J, M\rangle \quad \omega \rightarrow 0 \tag{2}$$

where $a_{JM}(\omega)$ is the coefficient, which specifies the eigenfunction as linear combination of all rotational levels in a vibrational state. For any fixed value of the good quantum number M, the range of J involved in this coherent superposition or hybrid wavefunction increases with the ω parameter. The eigenstates are labeled by M and the nominal value of $\tilde{J}$ of the angular momentum for the field-free rotor state that adiabatically correlates with the high-field hybrid function. For $\omega > 0$, the states with different values of |M| within each $\tilde{J}$ manifold have different energies[42]. For transitions between a pair of pendular states, $|\tilde{J}'', M'', \omega''\rangle \rightarrow |\tilde{J}', M', \omega'\rangle$, and the line-strength factor is given by[42]

$$\begin{aligned} S(\nu) &= P(J'') \times \sum_{J'', J', q} a^2_{J''M''}(\omega'') a^2_{J'M'}(\omega')(2J'' + 1)(2J' + 1) \\ &\times \begin{pmatrix} J'' & 1 & J' \\ -M'' & q & M' \end{pmatrix}^2 \begin{pmatrix} J'' & 1 & J' \\ 0 & 0 & 0 \end{pmatrix}^2 \end{aligned} \tag{3}$$

And the corresponding normalized integrated intensity of the Q-branch spectra is given by

$$I_Q(r, \nu_0) = \frac{\int_{-S_{Qmin}}^{+S_{Qmin}} S_Q(\nu) d\nu}{\int_{-S_{min}}^{+S_{min}} S(\nu) d\nu} \tag{4}$$

where ν is the vibratioanl transition frequency; $a_{J''}$ and $a_{J'}$ are the coefficients introduced by the field-induced hybridization of J' and J'' states give rise to non-zero transition probabilities between the states that differ by more than unity in their nominal $\tilde{J}$ value; $P(J'')$ is the relative population of initial thermal equilibrium, which meets the Maxwell-Boltzmann distribution. In our calculations, the redistribution process of molecules in the E-field was assumed as an adiabatic one, and thus $P(J'') = P(\tilde{J}'')$. q $(=0, \pm 1)$ designates the spherical components in the space-fixed frame of the E-field vector of the radiation. q = 0 means that the polarization of the probe beam is parallel to the direction of the E-field vector; q = ±1 means that these two directions are orthogonal each other. The relative strength $I_Q(r, \nu_0)$ of the "Q-branch" can be calculated by using Eq. (4), here ν_0 is the band origin. ± S_{Qmin} and ±S_{min} are the minimum values of the "Q-branch" and entire ro-vibrational spectra's both sides. The spectrum line profile was considered as Gaussian function, its full width at half maximum (FWHM) was set as B/4[43].

The spectra of possible rovibrational transitions of the ν_1 vibrational mode of C-H stretch of linear cyanoacetylene trimer $(HCCCN)_3$[43] in various applied E-field strengths (including $E = 0$) were calculated by using Eq. (3), and the results are shown in Fig. 2. Table 1 shows the three kinds of molecular parameters in our calculation. It is clear that our calculated parallel transition spectrum (see the left spectrum in Fig. 2) of $(HCCCN)_3$ molecule are similar to the experimental ones of $(HCN)_3$[3], HCCCN[16], $(HCCCN)_3$[18], and C_2H_4[44]. This shows that these experimental spectrums verify our calculated results (see Fig. 2).

We can see from Fig. 2 that there are only P- and R-branch transitions that are allowed in free external field, the Q-branch is forbidden [see Fig. 1]. However, the mixing of the wave functions of the linear molecules in the electric fields will lead to the appearance of so-called "Q-branch" forbidden lines in the laser induced fluorescence (LIF) spectra, and the intensity of the new coming "Q-branch" depends on the E-field strength. The calculated rotationally resolved spectra of $(HCCCN)_3$ under the parallel transition (the transitions of $\Delta M_J = 0$) and the perpendicular transition (the transitions of $\Delta M_J = \pm 1$) are showed in Fig. 2.

Figure 2 shows the change of the parallel and perpendicular transition rotational resolved spectra of $(HCCN)_3$ in different electric fields. In the left side of Fig. 2, a "Q-branch" is appear and its intensity rise with the increase of the E-field strength. The higher the E-field strength is, the stronger the "Q-branch" intensity will be, and the weaker the P-, R-branch intensities will be, and this process is going faster under a lower molecular rotational temperature (MRT). This shows that cold/ultracold molecules are more sensitive samples for measuring the strength of weak E-fields. In particular, we find that when the E-field is high enough, the P- and R-branch spectra will be nearly disappear, while there is only a single Q-branch spectrum. In Fig. 2, a multi-peak spectral structure appears in the Q-branch when the Stark interaction strength $\omega \equiv \mu E/B \geq 61$ for $(HCCCN)_3$ with a MRT of 1 K and rise with increasing the E-field strength, which is due to the slight difference of the electric dipole moments, μ, and molecular constants B of the upper and lower vibrational ground states, v and v″. To our knowledge, this multi-peak spectral structure is the first finding in the world. It is clear that such a multi-peak spectral structure can be used to precisely measure the electric dipole moments μ and B constants of the selected molecules. In the right side of Fig. 2, the P- and Q-branches show complicated structures and Stark shifts, and then they will finally collapse into two broad clumps with the increase of the E-field strength.

Q-branch integrated intensity of pendular-state spectrum. The integrated intensity of the Q-branch of $(HCCCN)_3$ under different E-field strength were calculated, and the dependence of the normalized intensity of the "Q-branch" of $(HCCCN)_3$ with different MRT on the E-field strength E was studied by using Eq. (4), and the results are shown in Fig. 3. From Fig. 3 we can see that with the increase of E-field strength, the integrated intensity of the Q-branch will be increased quickly, then raised slowly, and reached to a saturated value finally. Due to static Stark shift, higher rotational levels will be mixed in stronger E-field easily. The intensity of the Q-branch reaches its saturated value when all rotational levels were mixed. Moreover, when the E-field strength is increased

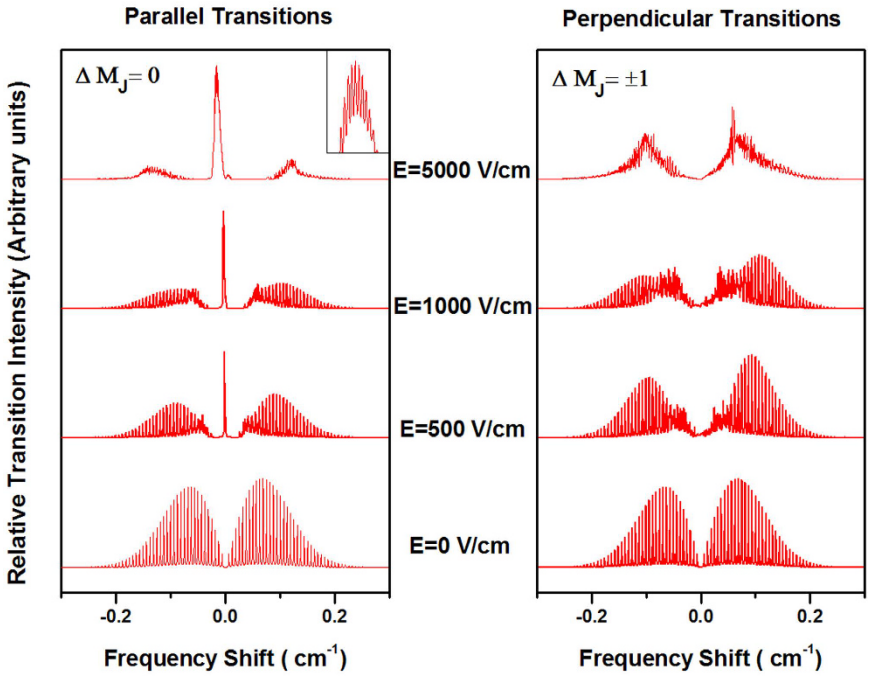

Figure 2. Calculated rotationally resolved spectrum of $(HCCCN)_3$ molecule based on the molecular constants listed in Table 1. The lower abscissa scale is in cm^{-1} relative to the band origin of the vibrational mode of C-H stretch.

Molecule	$\mu''(D)$	$\mu'(D)$	$B''(cm^{-1})$	$B'(cm^{-1})$	ω	$v_0(cm^{-1})$
$(HCCCN)_3$ [43]	11.4	11.67	0.00313654	0.00313626	61.03	3323.68245
HCN-N_2 [45]	3.04	3.085	0.052513	0.052138	0.972	3301.9389
HCl[42]	1.1085	1.139	10.44025	10.13623	0.00178	2885.9765

Table 1. Molecular parameters (μ, B) and values of $\omega = \mu E/B$ as E = 1 kV cm^{-1}.

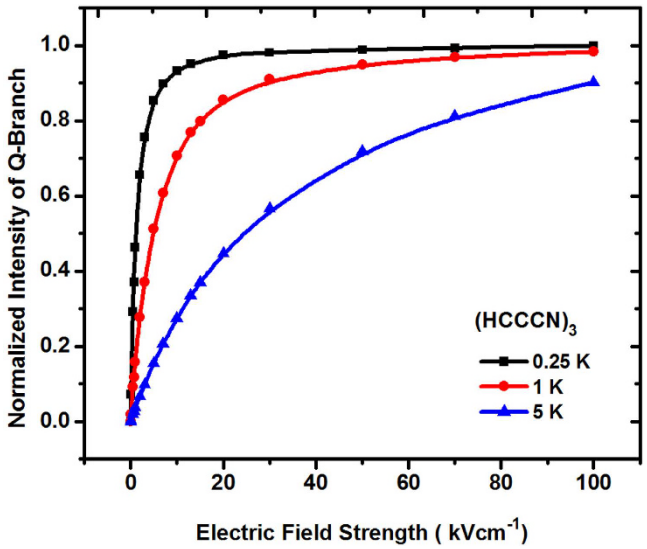

Figure 3. The dependences of the normalized Q-branch intensity on the E-field strength for different rotational temperature of $(HCCCN)_3$.

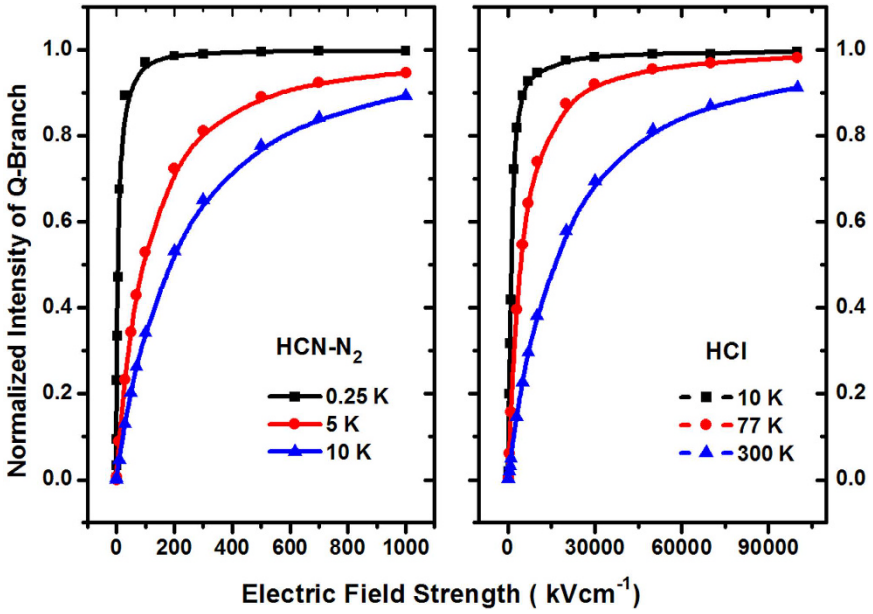

Figure 4. The dependences of the normalized Q-branch intensity of (left) HCN-N_2 and (right) HCl molecules on the E-field strength for different rotational temperature.

from 0 to 10 kV cm^{-1}, the intensity of the "Q-branch" of $(HCCCN)_3$ with a MRT of 0.25 K will be increased faster than that with a MRT of 5 K, and the low-energy rotational levels will be easily mixed in the E-field. This is because most of cold molecules are populated in lower rotational levels dominantly, thus the colder molecules will reach its saturation in the external E-field quickly, and has stronger relative intensity factor of Q-branch compared with that of a higher molecular temperature. In particular, when T = 0.25 K, the Q-branch integrated intensity of cold $(HCCCN)_3$ will be increased from 0 to about 0.95 when the E-field strength is increased from 0 to 10 kV cm^{-1}; while T = 5 K, it will be increased from 0 to ~0.90 with increasing E-field strength from 0 to 100 kV cm^{-1}.

We also investigate the dependence of the normalized integrated intensity of the Q-branch on the E-field strength for HCN-N_2 [45] and HCl[42], and the results are shown in Fig. 4. It is clear from Fig. 4(a) that when T = 5 K, the Q-branch integrated intensity of cold HCN-N_2 will be increased from about 0.3 to 0.95 when the E-field strength is increased from 50 kV cm^{-1} to 1000 kV cm^{-1}; while T = 10 K, it will be increased from about 0.35 to 0.90 with increasing the E-field strength from 100 kV cm^{-1} to 1000 kV cm^{-1}. Also, we can see from Fig. 4(b) that when T = 77 K (i.e., the liquid nitrogen (LN) temperature), the Q-branch integrated intensity of cold HCN-N_2 will be increased from about 0.35 to 0.98 when the E-field strength is increased from 5000 kV cm^{-1} to 10^5 kV cm^{-1}; while T = 300 K (i.e., the room temperature), it will be increased from about 0.3 to 0.92 with the increase of the E-field strength from 7500 kV cm^{-1} to 10^5 kV cm^{-1}. These results show that it is suitable to observe the Q-branch spectrum of cold linear $(HCCCN)_3$, HCN-N_2 and the room temperature HCl in a weak, moderate and strong E-field, respectively.

Figure 5 is the dependence of the normalized integrated intensity of $(HCCCN)_3$ Q-branch on the MRT T, and shows that for a certain E-field strength, with the reduction of the MRT, the intensity of Q-branch will be first increased and then slowly reached to a saturation value. Particularly, when T ≤ 1 mK, the E-field measurement value of ultracold $(HCCCN)_3$ can reach ~0.01 V cm^{-1}, even a smaller value. This is because the lower the MRT T is, the higher the population of lower rotational levels will be, and when the MRT T is low enough, the population of the lowest rotational level will reach its highest value, and then the integrated intensity of the Q-branch will reach its saturation value. This result shows that the lower the MRT is, the weaker the needed E-field will be, and ultracold linear molecules in a weaker E-field can be used to obtain a higher sensitivity for the observation of the Q-branch integrated intensity.

Discussion

Some potential applications. First, we can see from Fig. 2 that a newly-found multi-peak spectral structure can be used to precisely measure the electric dipole moments μ and B constants of different vibration states of cold linear molecules.

Secondly, it is clear from Figs 3, 4 and 5 that ultracold or cold $(HCCCN)_3$ with a temperature of lower or higher than 1 mK is suitable to measure a weaker E-field strength within 10^{-5} ~ 100 kV cm^{-1}, cold HCN-N_2 and heat HCl from 77 K to 300 K are suitable to measure a moderate E-field strength (1 ~ 10^3 kV cm^{-1}) and a strong one (10^2 ~ 10^5 kV cm^{-1}) by using the pendular Q-branch spectra of the linear molecule, respectively. The measurement principle and method will be introduced in some detail as follows: in our proposed scheme, the space of the measured E-field will be filled with the selected cold linear molecule gas, which can be generated by using buffer-gas cooling and Stark velocity filter[23,24] or Stark decelerator[22] in a high vacuum chamber. A tunable single-mode, linear-polarized probe beam from an OPO/OPA laser system is focused into the chamber and used to excite cold

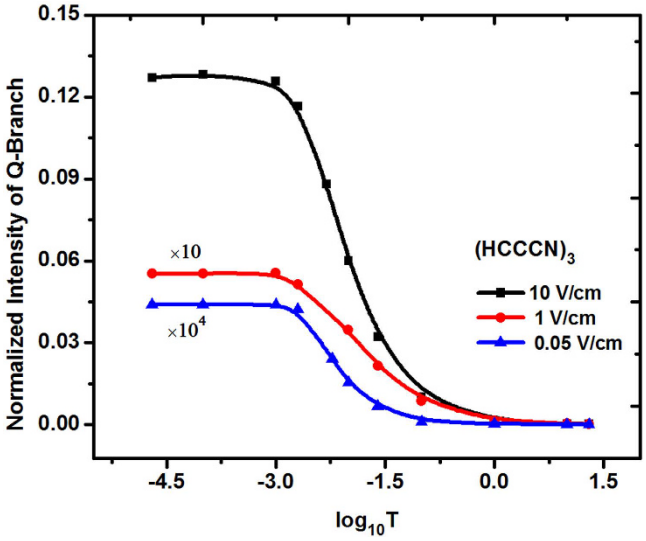

Figure 5. The dependences of the normalized Q-branch intensity on the rotational temperature of $(HCCCN)_3$ for different E-field strength. In which, the Y-coordinate values of the red and blue lines are multiplied by 10 times and 10000 times in order to compare with the black one; the line width of each possible transition is changed by 0.00001 cm^{-1} (≈B/300) to obtain higher resolution under 0.05 V cm^{-1}.

molecule sample so as to generate the fluorescence spectra of the rovibrational transitions, and the resulting LIF spectra will be collected and detected by an IR detector system. If the fluorescence collective coefficient η_{coll}, and the quantum efficiency η_{Det} of the detector were assumed as a constant near the band origin ν_0, the photoelectric current of the detected fluorescence intensity of the "Q-branch" can be given by

$$i_Q(r, \nu_0) = AP_0\eta_{coll}V\rho(r)\int_{-S_{\min}}^{+S_{\min}} \eta_{\det}(\nu)S_Q(\nu)d\nu \approx B(\nu_0)\rho(r)I_Q(r, \nu_0). \quad (5)$$

where $B(\nu_0) = AP_0\eta_{coll}\eta_{\det}$, A is the system coefficient, P_0 and V are the power of the probe beam and the effective probing volume, respectively. From Figs 3, 4 and 5, the measured E-field strength can be expressed as

$$E(r) = kI_Q(r, \nu_0) = ki_Q(r, \nu_0)/[B(\nu_0)\rho(r)]. \quad (6)$$

where k is the proportional coefficient, which can be determined by the Q-branch intensity of cold linear molecules in a homogeneous E-field generated by a pair of plate electrodes, that is, it can be determined by the calibration curve of the resulting Q-branch intensity of a plate capacitor. $\rho(r)$ is the spatial density distribution of cold molecules and will be easily affected by the E-field environment, but this problem can be solved by using a CCD camera to obtain the fluorescent intensity distribution from the molecule sample, which is proportional to the spatial density distribution of cold molecules in an entire measurement region. This is similar to the measurement method of cold atomic density used in the MOT or BEC experiments.

The basic principle for measuring the direction of the E-field vector can be simply described as follows: the magnitude and direction of the E-field vector in a two-dimensional (2D) plane (such as in XOY plane) can be measured by changing the direction of the probe-beam polarization two times. That is, from Eq. (6), when the direction of the probe-beam polarization is in the X direction, as shown in Fig. 6(a), the X component E_X of the measured E-field vector can be obtained by measuring the photon current i_{QX} from the corresponding LIF intensity I_{QX} of the Q-branch. If the direction of the probe-beam polarization is changed as the Y direction [see Fig. 6(b)], the Y component E_Y of the measured E-field vector will be obtained by measuring iQY from the corresponding I_{QY}. Then, the magnitude $|\vec{E}(r)| = \sqrt{E_X^2 + E_Y^2}$ of the measured E-field vector $\vec{E}$ in 2D space and its azimuthal angle $\theta = \arctan(E_Y/E_X)$ or $\theta = \pi - \arctan(E_Y/E_X)$ will be determined. Similarly, if the propagation direction of the probe beam is changed from the Z direction to the X or Y direction, and the direction of the laser polarization is changed to the Z direction, the Z component E_Z of the measured E-field vector can be determined by using similar measurement method, and then we can obtain the E-field vector $\vec{E}$ in 3D space.

Finally, it is well known that the stronger the electric field is, the higher the orientation degree of cold linear-molecules will be[1], so the dependence of Q-branch integrated intensity on the electric-field strength can also be used to measure the orientation degree of cold linear-molecules.

Measurement sensitivity. Similar to the derivation of measurement sensitivity expression in refs 46,47, when neglecting the inference of stray light on the measured LIF signal, the single-shot limited sensitivity of our method to measure the static electric field, determined by only shot noise resulting from the fluctuation of the fluorescence signal, is given by (see Supplementary material for more details)

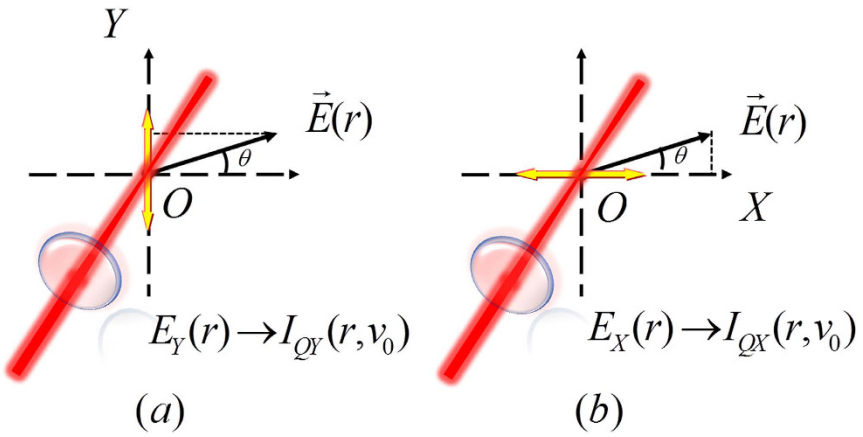

Figure 6. Schematic diagrams to measure (**a**) the Y component, $E_Y(r)$, and (**b**) the X component, $E_X(r)$, of the E-field vector. Yellow double arrow represents the polarization direction of the probe beam.

$$E(V/\mathrm{cm}) = \frac{1}{100}\frac{\sqrt{2}}{\sqrt{\kappa\eta n V_{eff}}}, \tag{7}$$

where η_c is the fluorescence collecting efficiency, n is the density of a supersonic molecular beam, and κ the front factor of E^2. The effective detected volume within probe laser beam can be assumed as a spheroid, it's volume V_{eff} equals to $\frac{4}{3}\pi a^2 b = \frac{8}{3}\pi w_0^2 f$, here w_0 is the waist radius, and f represents the Rayleigh length of the Gaussian beam. When the fluorescence collecting efficiency of detection system is $\eta_c = 10\%$, the rotational temperature of a supersonic $(HCCCN)_3$ beam is 5 K, and the waist radius of the focused probe beam is $w_0 = 10\,\mu$m, we obtain a static electric-field sensitivity of 2.05×10^{-7} V/cm[48]. It is clear that when SNR = 1, the relative measurement error (1/SNR, or measurement accuracy) reaches 100%. So in order to obtain a 1% relative measurement error (a relative uncertainty), the SNR should be equal to 100, and the corresponding practical sensitivity is $E = 2.05 \times 10^{-5}$ V/cm, which is far lower than ones (5 V/cm ~ 100 V/cm) of other methods[36,38,39].

Conclusion

We have calculated pendular-state spectra of cold linear molecules, and studied the dependences of the integrated intensity of the Q-branch on both the E-field strength and the MRT of cold linear molecules, and found that these dependences can be used to sensitively measure the E-field vector and its spatial distribution by changing the polarization directions of the focused probe-beam as well as the orientation degree of cold linear molecules. Also, we have found some new physical phenomena as follows: (1) the saturation effect of the integrated intensity of the Q-branch in a strong E-field; (2) the similar saturation effect occurred at an ultralow temperature of the linear molecules, and (3) a multi-peak structure in the Q-branch spectrum as well as its appearing condition $\omega \equiv \mu E/B \geq 61$ for $(HCCCN)_3$, and given reasonable physical explanations. Our study shows that the proposed measurement method can cover an ultrawide range of about $10^{-5}\,\mathrm{V\,cm^{-1}} \sim 10^{5}\,\mathrm{kV\,cm^{-1}}$ theoretically, and the corresponding practical measurement sensitivity is $2.05\ 10^{-5}\,\mathrm{V\,cm^{-1}}$. So it is clear that such a high-sensitive and ultrawide-range method can be used to realize the nonintrusive, *in-situ* measurement of the E-field vector and its spatial distribution in Stark decelerator[22], velocity filter[23,24], electrostatic guide[25] and beam splitter[26], and electrostatic trap[27], and so on [49]. Also, it can be used to measure the E-field vector and its spatial gradient in eEDM experiment using heavy-atom molecules (such as YbF, PbF and ThO, etc.)[30–33] because they have a larger EDM and a smaller B constant.

References

1. Friedrich, B. & Herschbach, D. R. Spatial orientation of molecules in strong electric fields and evidence for pendular states. *Nature* **353,** 412–414 (1991)
2. Rost, J. M., Griffin, J. C., Friedrich, B. & Herschbach, D. R. Pendular states and spectra of oriented linear molecules. *Phys. Rev. Lett.* **68,** 1299–1302 (1992).
3. Block, P. A., Bohac, E. J. & Miller, R. E. Spectroscopy of pendular states: The use of molecular complexes in achieving orientation. *Phys. Rev. Lett.* **68,** 1303–1306 (1992).
4. Friedrich, B. Electric dipole moments of pendular molecules. *International Rev. Phys. Chem.* **14,** 113–126 (1995).
5. Slenczka, A. Electric linear dichroism with a simple interpretation in terms of molecular pendular states. *Phys. Rev. Lett.* **80,** 2566–2569 (1998).
6. Moore, D. T., Oudejans, L. & Miller, R. E. Pendular state spectroscopy of an asymmetric top: Parallel and perpendicular bands of acetylene-HF. *J. Chem Phys.* **110,** 197–208 (1999).
7. Kanya, R. & Ohshima, Y. Pendular-limit representation of energy levels and spectra of symmetric- and asymmetric-top molecules. *Phys Rev. A* **70,** 013403 (2004).
8. Bulthuis, J., Becker, J. A., Moro, R. & Kresin, V. V. Orientation of dipole molecules and clusters upon adiabatic entry into an external field. *J. Chem. Phys.* **129,** 024101 (2008).
9. Durand, A., Loison, J. C. & Vigue, J. Hyperfine structure of pendular states and the sign of the dipole moment of ICl A state. *J. Chem. Phys.* **101,** 3514–3519 (1994).

10. Kim, W. & Felker, P. M. Ground-state intermolecular spectroscopy and pendular states in benzene-argon. *J. Chem. Phys.* **107,** 2193–2204 (1997)
11. Slenczka, A. Polarization spectroscopy of pendular molecules in the gas phase. *Chem. Eur. J.* **5,** 1136–1143 (1999).
12. Oudejans, L., Moore, D. T. & Miller, R. E. state-to-state vibrational predissociation dynamics of the acetylene-HF complex. *J. Chem. Phys.* **110,** 209–219 (1999).
13. Franks, K. J., Li, H. & Kong, W. Orientation of pyrimidine in the gas phase using a strong electric field: Spectroscopy and relaxation dynamics. *J. Chem. Phys.* **110,** 11779–11788 (1999).
14. Kanya, R. & Ohshima, Y. Pendular-state spectroscopy of the S1-S0 electronic transition of 9-cyanoanthracene. *J. Chem. Phys.* **121,** 9489–9497 (2004).
15. Durand, A., Loison, J. C. & Vigue, J. Spectroscopy of pendular states: Determination of the electric dipole moment of ICl in the $X^1\sum^+(v''=0)$ and $A^3\Pi_1(v'=6–9)$ levels. *J. Chem. Phys.* **106,** 477–484 (1997).
16. Stiles, P. L., Nauta, K. & Miller, R. E. Dipole moments of molecules solvated in Helium Nanodroplets. *Phys. Rev. Lett.* **90,** 135301 (2003).
17. Kanya, R. & Ohshima, Y. Determination of dipole moment change on the electronic excitation of isolated Coumarin 153 by pendular-state spectroscopy. *Chem. Phys. Lett.* **370,** 211–217 (2003).
18. Nauta, K., Moore, D. T. & Miller, R. E. Molecular orientation in superfluid liquid helium droplets: high resolution infrared spectroscopy as a probe of solvent-solute interactions. *Faraday Discuss* **113,** 261–278 (1999).
19. Rudic, S., Merritt, J. M. & Miller, R. E. Study of the CH_3···H_2O radical complex stabilized in helium nanodroplets. *Phys. Chem. Chem. Phys.* **11,** 5345–5352 (2009).
20. Wei, Q., Kais, S., Friedrich, B. & Herschbach, D. Entanglement of polar molecules in pendular states. *J. Chem. Phys.* **134,** 124107 (2011).
21. Shvartsburg, A. A., Noskov, S. Y., Purves, R. W. & Smith, R. D. Pendular protein in gases and cew avenues for characterization of macromolecules by ion mobility spectrometry. *PNAS* **106,** 6495–6500 (2009).
22. Bethlem, H. L., Berden, G. & Meijer, G. Decelerating neutral dipolar molecules. *Phys. Rev. Lett.* **83,** 1558–1561 (1999).
23. van Buuren, L. D. *et al.* Electrostatic extration of cold molecules from a cryogenic reservoir. *Phys. Rev. Lett.* **102,** 033001 (2009).
24. Liu, Y., Yun, M., Xia, Y., Deng, L. & Yin, J. Experimental generation of a cw cold CH_3CN molecular beam by a low-pass energy filtering. *Phys. Chem. Chem. Phys.* **12,** 745–752 (2010).
25. Xia, Y., Yin, Y., Chen, H., Deng, L. & Yin, J. Electrostatic surface guiding for cold polar molecules: experimental demonstration. *Phys. Rev. Lett.* **100,** 043003 (2008).
26. Deng, L. *et al.* Experimental demonstration of a controllable electrostatic molecular beam splitter. *Phys. Rev. Lett.* **106,** 140401 (2011).
27. Bethlem, H. L. *et al.* G. Electrostatic trapping of ammonia molecules. *Nature* **406,** 491–494 (2000).
28. Shuman, E. S., Barry, J. F., Glenn, D. R. & DeMille, D. Radiative force from optical cycling on a diatomic molecule. *Phys. Rev. Lett.* **103,** 223001 (2009).
29. Hummon, M. T. *et al.* 2D magneto-optical trapping of diatomic molecules. *Phys. Rev. Lett.* **110,** 143001 (2013).
30. Hudson, J. J. *et al.* Improved measurement of the shape of the electron. *Nature* **473,** 493–496(2011)
31. Shafer-Ray, N. E. Possibility of 0-g-factor paramagnetic molecules for measurement of the electron's electric dipole moment. *Phys. Rev. A* **73,** 034102 (2006).
32. Eckel, S., Hamilton, P., Kirilov, E., Smith, H. W. & DeMille, D. Search for the electron electric dipole moment using _-doublet levels in PbO. *Phys. Rev. A* **87,** 052130 (2013).
33. Baron, J. *et al.* Order of Magnitude Smaller Limit on the Electric Dipole Moment of the Electron. *Science* **343,** 269 (2014)
34. Macintyre, S. A. *Magnetic Field Measurement* (CRC Press LLC, 1999)
35. Ise, T., Tsukizaki, R., Togo, H., Koizumi, H. & Kuninaka, H. Electric field measurement in microwave discharge ion thruster with electro-optic probe. *Rev. Sci. Instrum.* **83,** 124702 (2012).
36. Doughty, D. K. & Lawier, J. E. Spatially resolved electric field measurements in the cathode fall using optogalvanic detection of Rydberg atoms. *Appl. Phys. Lett.* **45,** 611–613 (1984).
37. Stevens, G. D., Iu, C.-H., Bergeman, T. & Metcalf, H. J. Precision measurements on lithium atoms in an electric field compared with *R*-matric and other Stark theories. *Phys. Rev. A* **53,** 1349–1366 (1996).
38. Moore, C. A., Davis, G. P. & Gottscho, R. A. Sensitive, nonintrusive, *In-Situ* measurement of temporally and spatially resolved plasma electric fields. *Phys. Rev. Lett.* **52,** 538–541 (1984).
39. Czarnetzki, U., Luggenholscher, D. & Dobele, H. F. Sensitive electric field measurement by fluorescence-dip spectroscopy of Rydberg states of atomic hydrogen. *Phys. Rev. Lett.* **81,** 4592–4595 (1998).
40. Slinker, J. D. *et al.* Direct measurement of the electric-field distribution in a light-emitting electrochemical cell. *Nature Materials* **6,** 894–899 (2007).
41. Zhu, L. *et al.* Measurement of polarization-induced electric fields in GaN/AlInN quantum wells. *Appl. Phys. Lett.* **101,** 251902 (2012)
42. Friedrich, B. *et al.* Optical spectra of spatially oriented molecules: Icl in a strong electric field. *J. Chem. Soc. Faraday Trans.* **89,** 1539–1549 (1993).
43. Yang, X., Kerstel, E. R. Th., Scoles, G., Bemish, R. J. & Miller, R. E. High resolution infrared molecular beam spectroscopy of cyanoacetylene cluster. *J. Chem. Phys.* **103,** 8828–8239 (1995).
44. Sanzharov, M. *et al.* Stark spectrum simulation for X_2Y_4 molecules: Applcation to the ν_{12} band of ethylene in a high-silica zeolite, *J. Chem. Phys.*, **136,** 134314 (2012).
45. Jucks, K. W. & Miller, R. E., SubDoppler resolution infrared spectra of the isoelectronic pair: N_2-HCN and OC-HCN. *J. Chem. Phys.* **89,** 1262–1267 (1988).
46. Alyabyshev, S. V., Lemeshko, M. & Krems, R. V., Sensitive imaging of electromagnetic fields with paramagnetic polar molecules. *Phys. Rev. A.* **86,** 013409 (2012)
47. Böhi, P., Riedel, M. F., Hänsch, T. W. & Treutlein, P., Imaging of microwave fields using ultracold atoms. *Appl. Phys. Lett.* **97,** 051101 (2010).
48. van de Meerakker, S. Y. T., Bethlem, H. L., Vanhaecke, N. & Meijer, G., Manipulation and control of molecular beams. *Chem. Rev.* **112,** 4828–4878 (2012).

Acknowledgements

We gratefully acknowledge support for this work by the National Nature Science Foundation of China under Grant Nos 91536218, 10674047, 10804031, 10904037, 10974055, 11034002, 11205198, 61205198, and 11274114, the Fundamental Research Funds for the Central Univesities, the National Key Basic Research and Development Program of China under Grant No. 2011CB921602.

Author Contributions

J.Y. conceived the idea, and M.D. did the theoretical calculations , the numerical simulations and wrote the manuscript. H.W. and Q.W. checked it.

Additional Information

Supplementary information accompanies this paper at http://www.nature.com/srep

Competing financial interests: The authors declare no competing financial interests.

How to cite this article: Deng, M. *et al.* Dependences of Q-branch integrated intensity of linear-molecule pendular spectra on electric-field strength and rotational temperature and its potential applications. *Sci. Rep.* **6**, 26776; doi: 10.1038/srep26776 (2016).